Environmental Science and Pollution Research (2022) 29:27195–27208
https://doi.org/10.1007/s11356-021-17699-6

RESEARCH ARTICLE

The Whitehill Formation as a natural geochemical analogue to the Witwatersrand Basin's mine water issues, South Africa

Dikeledi Tryphina Mashishi[1] · **Christian Wolkersdorfer**[1,2] · **Henk Coetzee**[3]

Received: 1 February 2021 / Accepted: 18 November 2021 / Published online: 3 January 2022

Abstract

Mining activities within the Witwatersrand Basin, South Africa, have led to many studies, particularly focusing on the generation of acid mine drainage (AMD) in the basin and the associated environmental effects. This study assesses whether gypsum in the Whitehill Formation is connected to acid rock drainage (ARD) resulting from reactions between the pyrite-bearing shale and carbonaceous rocks. To investigate this, the geochemical, geological and palaeoclimatic settings were investigated and a laboratory experiment with Whitehill Formation rock samples was conducted. XRF data of the rocks and modal analysis were used to determine the mineral composition of the Whitehill Formation. In addition, pH-redox equilibrium (PHREEQC) modelling was used for simulations. The results of this study show that metals precipitated from the water–rock solution form various mineral phases like those of the Witwatersrand Basin. Large-scale dolomite dissolution might not be expected.

Keywords Witwatersrand Basin · Mining influenced water (MIW) · Natural analogue · Whitehill Formation · Similar strata · Geochemical modelling

Introduction

South Africa's Witwatersrand Basin is one of the world's largest gold repositories, deposited between 2985 and 2849 Ma ago (McCarthy 2006). The rocks of the Witwatersrand Supergroup predominantly outcrop in the West Rand and Central Rand Goldfields. Limited outcrops are in the East Rand Goldfield, where the Witwatersrand sub-outcrops below dolomite and other sedimentary rocks of the Proterozoic Transvaal Supergroup and sedimentary rocks of the Permian Karoo Supergroup. Locally, these goldfields are commonly referred to as the Western, Central and Eastern Basins. To the east of this, the Witwatersrand sub-outcrops below younger Karoo sedimentary cover in the Evander Goldfield, while to the west and south, the Witwatersrand sub-outcrops below younger rocks, including an important karst aquifer system in the Far West Rand and KOSH (Klerksdorp-Orkney-Stilfontein-Hartbeesfontein) Goldfield and under Karoo cover in the Free State Goldfield (Johnson et al. 2006) (Fig. 1).

Mining influenced water (MIW, in this paper, the term MIW will be preferred over AMD, as MIW includes acidic as well circum-neutral mine water from the Witwatersrand Basins) of the Western, Central and Eastern Basins poses a risk to the local environment and to regional water security (Department of Water Affairs and Forestry South Africa 2009), while treated mine water in the Western Basin flows towards the Hominid Caves of Southern Africa Word Heritage Site (locally called "Cradle of Humankind"), where it recharges the Malmani dolomite aquifer (Hobbs 2008;

Responsible Editor: Philippe Garrigues

This paper is based on the first author's master thesis at Tshwane University of Technology and a preliminary presentation of the results at an IMWA (International Mine Water Association) conference.

✉ Christian Wolkersdorfer
christian@wolkersdorfer.info

Dikeledi Tryphina Mashishi
tryphinadmashishi@gmail.com

Henk Coetzee
henkc@geoscience.org.za

[1] Department of Environmental, Water and Earth Sciences, Tshwane University of Technology (TUT), Private Bag X680, Pretoria 0001, South Africa

[2] Laboratory of Green Chemistry, Lappeenranta University of Technology, Sammonkatu 12, 50130 Mikkeli, Finland

[3] Council for Geoscience, Private Bag X112, Pretoria 0001, South Africa

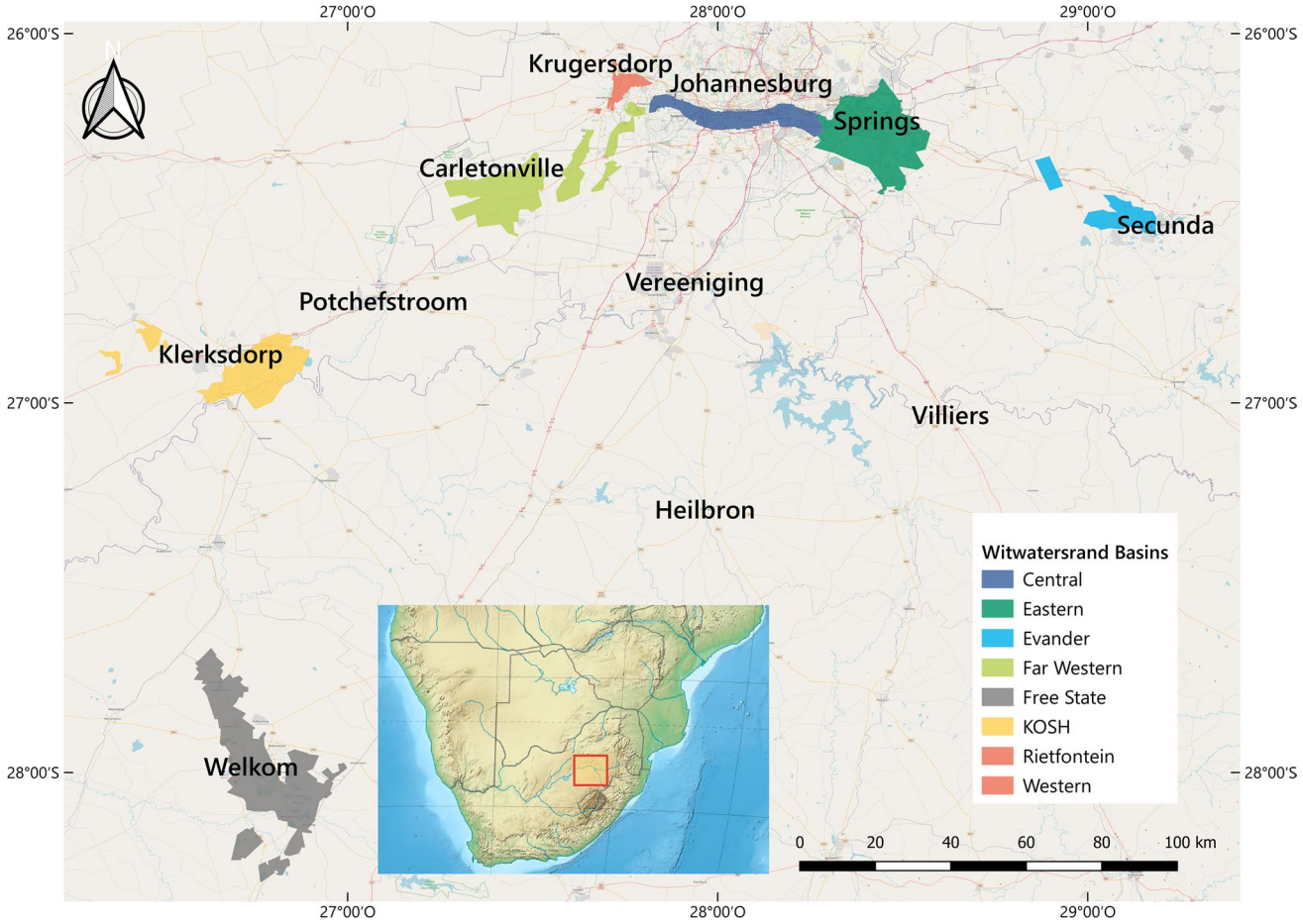

Fig. 1 Locality of the goldfields of the Witwatersrand; KOSH, Klerksdorp-Orkney-Stilfontein-Hartbeesfontein (service layer credits: OpenStreetMap Community, Eric Gaba, Wikimedia Commons user Sting)

Hobbs and Cobbing 2007; Hobbs et al. 2011). Although formal mining has declined in recent years, the negative effects of MIW from underground workings, stockpiles and waste rock dumps remain point sources (Coetzee 2013; Expert Team of the Inter-Ministerial Committee 2010).

This paper uses the Whitehill Formation of South Africa's Karoo Basin as a natural analogue to the mine water situation in the Witwatersrand. It will derive conclusions drawn from the natural analogue in relation to the mine water situation in the Witwatersrand mine water basins and the Hominid Caves of Southern Africa World Heritage Site.

Background

South Africa is a water-scarce country having recorded a deteriorating quality of freshwater resources (Expert Team of the Inter-Ministerial Committee 2010; Republic of South Africa and Department of Water Affairs and Forestry 2004). Mining, in particular gold and coal mining, has had a severe negative effect on water resources in some parts of South Africa, including the Witwatersrand Goldfield (McCarthy 2011; Naicker et al. 2003). Water resources near mining sites are often affected by the generation of acid mine drainage (AMD) which results from the oxidation of di-sulfides, such as pyrite or marcasite (FeS_2), by water and oxygen (Boukhalfa and Chaguer 2012; Geller et al. 1998; Liang-qi et al. 2010; Singer and Stumm 1970). This pyrite oxidation releases acidity and ferrous iron, which, after further reaction with oxygen, hydrolyses and produces ferric iron oxyhydroxide precipitates. The rate at which these redox reactions continue is determined by the microbial activity and the availability of the educts (Singer and Stumm 1970; Stumm and Morgan 1996; Younger et al. 2002).

To investigate the described processes and project them into the future, a natural analogue study was used. Analogues with similar but not entirely identical characteristics (Wolkersdorfer et al. 2020) are means to interpret the long-term behaviour of processes from one site and illustrate how it may be applicable to another one (Libourel et al. 2011; Miller et al. 2000). Identification of a site that has the potential as a natural analogue is based on similarity with a single

character or the same set of components (Choi et al. 2012). Yet, the "only problem is to find the proper ones" (Kesserü 1994). A common tool used in the investigation of MIW issues are laboratory experiments including but not limited to monitoring the concentration of metals and acid generation of a study site (Miller et al. 2000), which only lasts from days, weeks to months at most, which does not fully elucidate what happened in the past and what is likely to happen in the future (McCarthy 2011; Wolkersdorfer 2008). Nevertheless, the use of analogue studies also has drawbacks such as the difficulty of modelling because most natural systems are complex and involve complex processes (Miller et al. 2000). Yet, analogue systems can be used to interpret the slow natural mechanism that mimics those of an affected site at accelerated rates. To overcome the drawbacks of every single method, this study uses a combination of field and laboratory experiments (Smellie et al. 1997).

Strata similar to the Whitehill Formation also exist in the United States of America (USA), Germany, Paraguay, Uruguay as well as Brazil (Enomoto et al. 2012; Kern et al. 2008; Mathur et al. 2012; Rimmer 2004; Soares 2003). One of their key indicators is gypsum precipitates identified at the Tacuary Formation (Paraguay), Barnett Shale Formation (USA), Kupferschiefer Shale Formation (Germany) and the Marcellus Formation (USA) (Chukwuma and Bordy 2016; Geel et al. 2015; McLachlan and Anderson 1977; Oelofsen 1987).

Physical, chemical and biological processes in nature promote changes in sedimentary rocks. Factors controlling the rate and reaction of rock diagenesis are pore water composition, time, temperature and sedimentary facies (Berner 1980; Selley 2000). Generally, as pore water moves very slowly, it is highly mineralised, while groundwater flows faster and normally is less mineralised (Chapman 1981). Investigating the paleoclimate and chemical weathering of the study area was relevant to identify the degree to which the Whitehill Formation weathers and which long-term water–rock interactions might occur in the mining environment. Because of these interactions, chemical weathering transforms elements from a primary phase to secondary products (Hem 1985; Nesbitt and Markovics 1997; Nesbitt and Young 1982, 1989), sometimes called efflorescent salts (Jambor et al. 2000). A geochemical code is a tool used to gain an understanding of the geochemical processes of water–rock interactions and to make predictions of long-term behaviour that is commonly not achievable in experiments. For this study, the validation of long-term safety analysis of MIW was performed using the geochemical code PHREEQC to predict water–rock interactions, simulate the mineral dissolution and precipitation reactions based on observations in the field and laboratory experiments (Crawford 1999; Parkhurst and Appelo 2013).

The Whitehill Formation was identified as a potential analogue to portions of the Witwatersrand due to the observed similarities between the reaction products created when pyrite and dolomite weather, which occurs as concretions in the shale reacted, forming gypsum and staining the surrounding rock (Geel et al. 2015).

Methods

Description of the study area

The study area is located in South Africa's Northern and Western Cape provinces (Fig. 2), with two locations in the Northern Cape, Calvinia and Loeriesfontein (locations CV, LF1 and LF2), and one in the Western Cape, Laingsburg

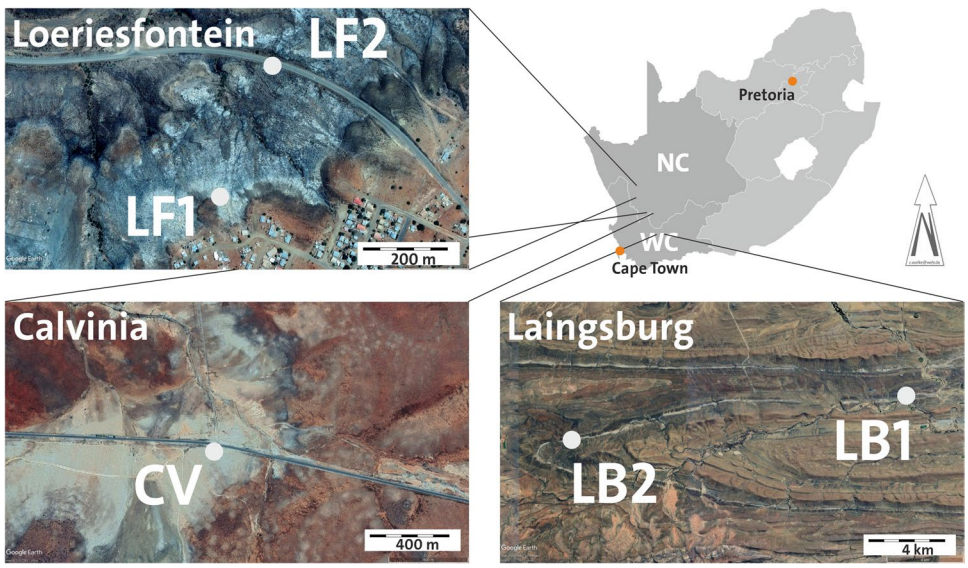

Fig. 2 Maps of the study area in north-western South Africa. NC, Northern Cape; WC, Western Cape (aerials © GoogleEarth)

(locations LB1 and LB2) (Supplementary Table S6). During fieldwork, the Whitehill Formation was carefully observed to describe the lithology, sedimentary features and collect rock samples for analysis.

Sampling, sample preparation and analysis

Four fresh (LF1a, LF2b, LB1 and LB2) and three weathered (LF1b, LF2a and CV) Whitehill Formation samples were collected from a layered sequence of thinly bedded dark grey-brown to black carbonaceous shale units. Rock samples were taken from the individual outcrops by using a geologist's hammer (Estwing E3/22P), ensuring to get a representative sample for the outcrop. Some samples were analysed for major elemental rock composition (PANalytical Axios X-ray fluorescence spectrometer [XRF] with 4 kW Rh tube, Council for Geoscience, Pretoria) with rock samples having been milled (< 75 µm fraction) and roasted at 1000 ℃ for > 3 h to oxidise Fe^{2+} and S and to determine the loss of ignition (LOI). Thereafter, 1.5 g of the roasted sample was fused on glass discs and 9 g of the flux consisting of 49.50% $Li_2B_4O_7$, 49.50% of $LiBO_2$ and 1.00% LiBr at 950 ℃. For trace element analysis, 12 g of the milled sample and 3 g of Hoechst wax were mixed and pressed into a powder briquette (25 kPa hydraulic press).

Modal analysis ("normative mineralogy") was used to determine the Whitehill Formation's mineral composition. Although the weakness of the CIPW norm for sedimentary rocks is known, the bulk chemical analysis results were used to estimate the rock's mineralogical composition (Doveton 2018; Jacobs et al. 2014; Le Maitre et al. 2002; Pruseth 2009). In addition, published data and field observations were used to evaluate the mineralogical composition. Calculation of hydrogen carbonate in the batch samples was conducted by subtracting the sum concentrations of anions from the cations.

Rock samples were split into pieces of 3–4 cm, weighed, placed in 500 mL beakers with 400 mL of distilled water to analyse and monitor changes of pH and electrical conductivity (EC) and kept in the dark. Monitoring proceeded over 12 weeks, using a Hach pHC201 pH- and a CDC401 EC-probe with a Hach HQ40d meter. Probes were calibrated daily with NIST traceable standard solutions (pH 4.01, 7.00, 10.01, EC 1413 µS/cm standard). Syringe-filtered samples were collected (0.45 µm nylon membrane), and the concentrations were measured by inductively coupled plasma-optical emission spectrometry [ICP-MS; Waterlab (Pty) Ltd Pretoria].

The degree of chemical weathering was estimated with the chemical index of alteration (CIA) (Nesbitt and Young 1982), where molar proportions of the major oxides were used and CaO* is the CaO incorporated in the silicate fraction of the rock (Eq. (1)). Additional geochemical proxy signals used were Rb/K, V/Cr and Zr/Ti. The concentration of elements Rb, K and Zr was divided by the concentration of K, Cr and Ti, respectively, to determine the ratios.

$$\mathrm{CIA} = \frac{\mathrm{Al_2O_3}}{\mathrm{Al_2O_3} + \mathrm{CaO^*} + \mathrm{Na_2O} + \mathrm{K_2O}} \cdot 100 \quad (1)$$

Modelling of the MIW environment was done using the chemical thermodynamic code PHREEQC (Parkhurst and Appelo 2013) (WATEQ4F database) to determine potential phase equilibria and focusing on Fe, Ca, Mg and SO_4^{2-} precipitates because of the gypsum found in the field. Possible mineral equilibria were determined using the calculated saturation indices (SI).

Principal component analysis (PCA), including the scatter and Biplot diagram, was conducted with the statistical software PAST 4.02 (Hammer et al. 2001) and the Pearson correlation with IBM SPSS Statistics 25.

Results

Geological setting

The weathered outcrops of the Whitehill Formation in Loeriesfontein consist of a fine-grained and well-laminated layer of dark grey shale, succeeded by layers of iron oxyhydroxide and gypsum on top. These layers are followed by a grey-brownish shale layer interbedded with iron oxyhydroxide and gypsum layers, then underlain by a grey shale layer and finally brownish shale interbedded with gypsum. The colour of the fresh carbonaceous shale is black. Dissolution of di-sulfide minerals generates acidity and sulfate which reacts with carbonates (e.g. calcite, ankerite, dolomite), producing Ca- and Mg-rich hydrogen carbonate fluids to precipitate gypsum, which outcrops, for example, at Calvinia and Loeriesfontein (Figs. 3 and 6). At the second outcrop in Loeriesfontein (LF2), up to 1 m long and 50 cm high dolomite concretions are interbedded in the black shales (Fig. 4), as also described in previous studies (Loeriesfontein and Jansenville) (Geel et al. 2015; Smithard et al. 2015). There, the carbonate concretions also contain large carbonate and gypsum crystals in vertical and horizontal fractures, particularly siderite ($FeCO_3$) as well as iron oxyhydroxide layers and gypsum grains of approximately 1–6 cm in size, associated with fluid movement from rock and mineral weathering processes. In addition, a fresh black shale with iron oxyhydroxide nodules of approximately 5 cm and iron hydroxide layers were identified (Fig. 5), also indicating oxidation reactions. A distinction of the black carbonaceous shale with greyish-white and yellow-brownish sugar-sized gypsum grains was identified (Fig. 6).

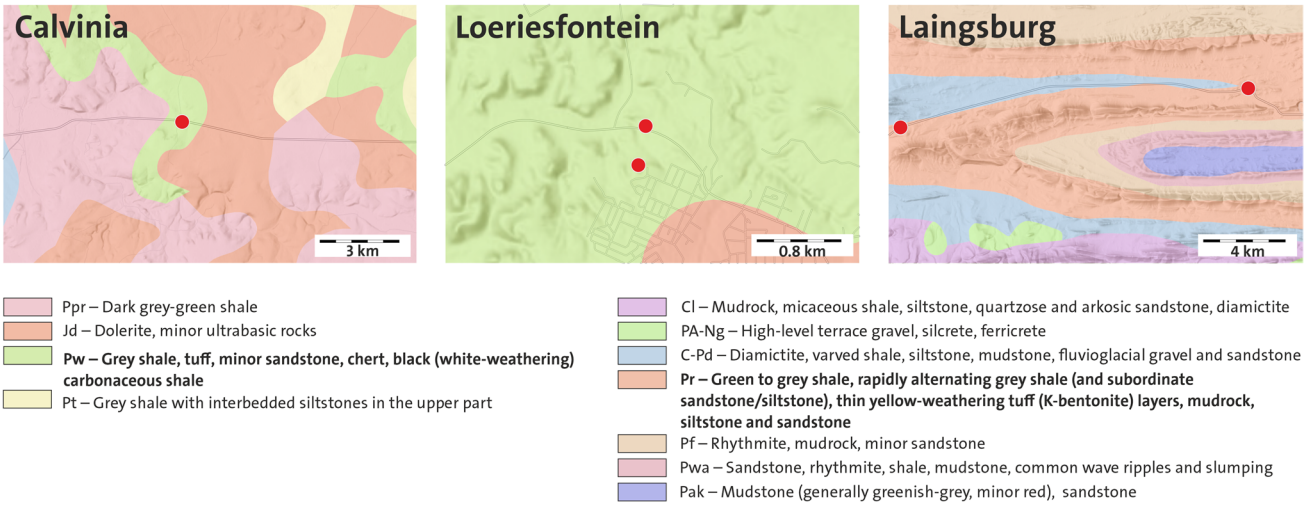

Fig. 3 Geological maps of the study areas in Calvinia, Loeriesfontein and Laingsburg (CGS 2019 data, Geological Map 1:1 Mio). Geological units that include the Whitehill Fm. are shown in bold. The left legend belongs to the Calvinia and Loeriesfontein maps; the right legend is to the Laingsburg map (C-Pp also to Calvinia)

Fig. 4 Carbonate concretion at location LF2 with white gypsum surrounding the concretion (scale: 40 cm)

Fig. 5 Iron oxyhydroxide crust at location LF1. Scale is in centimetres

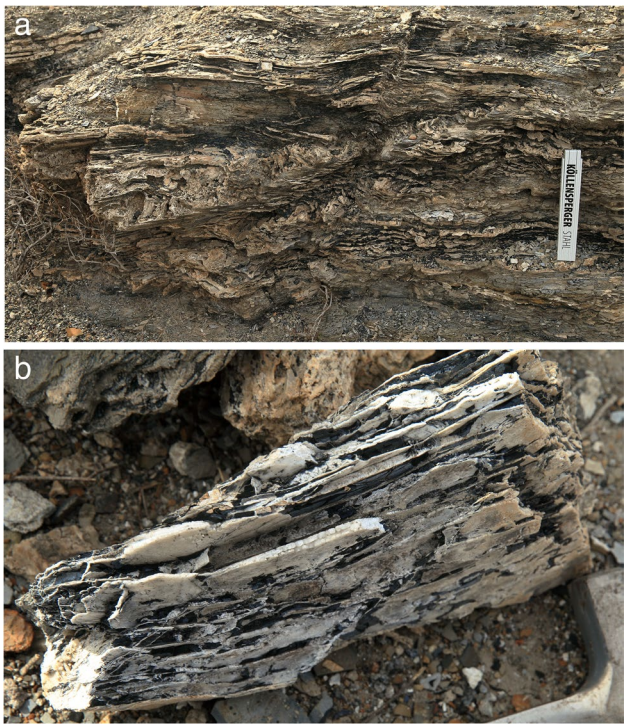

Fig. 6 Black carbonaceous shale intercalated with gypsum at LF1. Scale: 20 cm; right width: 20 cm

In Calvinia (CV; Supplementary Figure S1), the outcrop is characterised by basaltic rocks at its top (Supplementary Figure S2) and is underlain by a highly weathered greyish-white and iron oxyhydroxide layer. The underlying layer consists of well-folded layers of hard and dark-coloured coarse-grained black shales getting thicker from west to east,

contrasting with the soft and light-coloured iron-rich and highly weathered white gypsum layers and fibrous gypsum (satin spar) crystals (Fig. 7). In addition, the bottom layer is a black carbonaceous shale in contrast to the iron oxyhydroxide layer. Carbonate concretions of various sizes and shapes occur randomly at Laingsburg and are filled with pebble fractures indicating the effects of weathering agents on the rock (Supplementary Figure S3). Also observed at this site were milky quartz and chert (SiO_2), hard and resistant to weathering.

Geochemical analysis

Major and trace elements were used to describe the geochemical composition of the Whitehill Formation and to correlate it with processes that occur in AMD/MIW environments (Table 1). As expected, an opposite trend for SiO_2 and CaO and MgO concentrations in the rocks was observed (Supplementary Figure S4), and two groups could be identified by PCA (Fig. 8): samples LF1b, LF2a, CV were found to have higher contents of CaO (29.87 wt %) and MgO (21.34 wt %), which correspond to the presence of carbonates, whereas samples LF1a, LF2b, LB1 and LB2 have higher SiO_2 contents (88.93 wt %), corresponding with the presence of quartz, chert and silicates. The Pearson correlation coefficient (Table 2, Supplementary Table S7) analysis revealed a strong correlation between CaO, MgO, P_2O_5 and LOI. Calculation of the Cross, Iddings, Pirsson and Washington (CIPW) norm (Table 3) showed that the rocks' composition is dominated by calcite for samples LF1b, LF2a and CV, whereas quartz dominates samples LF1a, LB1 and LB2.

Batch experiments were conducted for investigating the development of aqueous solutions and analysis of the residual metal ion concentration therein. The pH of the seven batch samples analysed in the laboratory ranged between 3.55 and 8.14 and the EC between 0.07 mS/cm and 8.3 mS/cm (Fig. 9). Samples CV, LF1b and LF2a developed low pH values in the Fe to Al buffer range and high electrical conductivities, while samples LF1a, LF2b, LB1 and LB2 showed circum-neutral pH values and low electrical conductivities. The experiment was paused between December 2015 and January 2016. Results of chemical analysis showed (Table 4) that samples within the iron-buffer range had high concentrations of Ca, Mg and SO_4^{2-}, yet low Si concentrations, and samples with a circum-neutral pH had low concentrations of Ca, Mg and SO_4^{2-} and high Si concentrations.

Fig. 7 2-cm thick fibrous gypsum (satin spar) precipitates under a dolomite concretion at location CV. Scale in centimetres

Table 1 XRF analysis results for major element composition (wt %)

Parameter	LF1a	*LF1b*	*LF2a*	LF2b	*CV*	LB1	LB2
SiO_2	63.89	3.79	4.04	50.30	1.31	88.93	79.64
TiO_2	0.51	0.04	0.05	0.81	0.02	< 0.01	0.12
Al_2O_3	13.77	1.02	1.43	14.47	0.59	0.44	10.40
Fe_2O_3 (t)	4.76	4.28	5.32	10.96	0.27	3.40	1.21
FeO*	4.28	3.85	4.79	9.86	0.24	3.06	1.09
MnO	< 0.01	0.16	0.17	0.18	0.05	0.01	0.07
MgO	0.59	18.06	16.60	9.00	21.34	0.22	< 0.01
CaO	0.25	28.74	29.27	10.21	29.87	3.62	1.46
Na_2O	1.67	< 0.01	< 0.01	2.12	< 0.01	< 0.01	5.80
K_2O	3.77	0.09	0.12	0.25	0.04	0.02	0.16
P_2O_5	0.09	0.28	0.14	0.14	0.21	0.04	0.08
Cr_2O_3	0.01	0.01	0.01	0.08	< 0.01	0.04	0.02
LOI	10.74	43.40	42.91	1.14	46.42	3.43	1.13
H_2O	1.73	0.44	0.41	0.63	0.24	0.22	0.17
Total	100.05	99.88	100.06	99.66	100.12	100.16	100.09

Weathered samples resulting in acidic drainage in the batch experiments are in italics

t, iron oxidised in the + III state; *FeO**, calculated from Fe_2O_3; *LOI*, loss of ignition; *H_2O*, moisture water

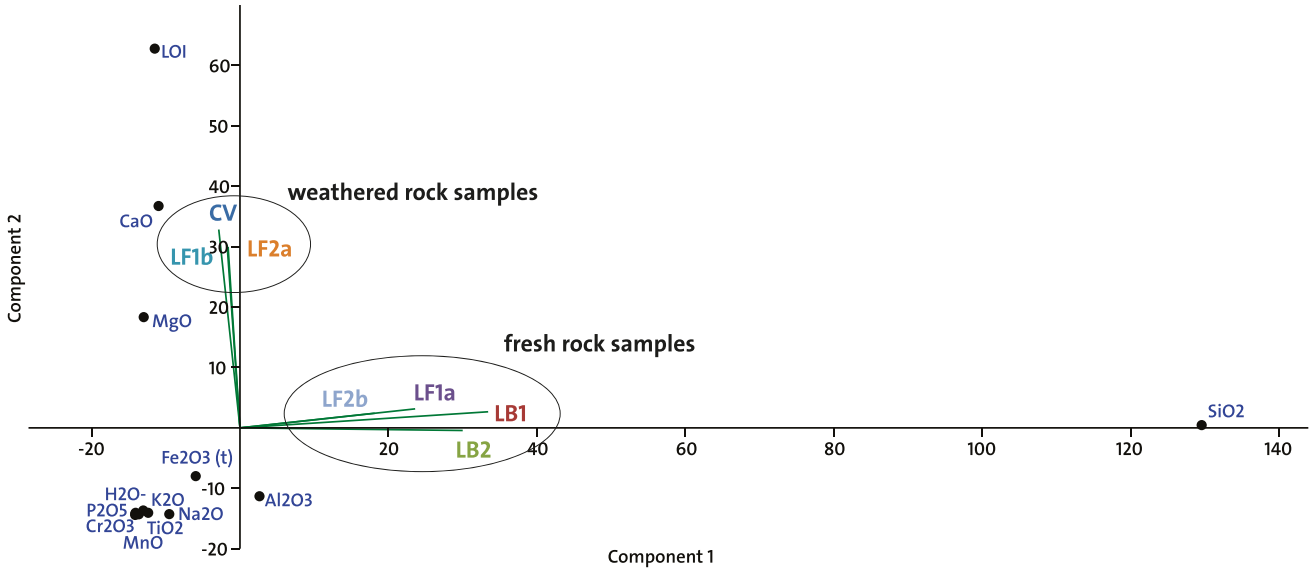

Fig. 8 Scatter diagram and Biplot of the principal component analysis of the XRF data

Table 2 Pearson correlation coefficients between the major oxides

	TiO_2	Al_2O_3	Fe_2O_3	MnO	MgO	CaO	Na_2O	K_2O	P_2O_5	Cr_2O_3	LOI	H_2O
SiO_2	0.26	0.49	0.04	**−0.56**	**−0.97**	**−0.97**	**0.56**	0.26	**−0.86**	0.47	**−0.94**	0.15
TiO_2		**0.87**	**0.80**	0.18	−0.29	−0.43	0.28	0.45	−0.17	**0.65**	−0.93	**0.59**
Al_2O_3			**0.50**	−0.04	**−0.55**	**−0.67**	**0.67**	**0.57**	−0.37	0.45	−0.69	**0.60**
Fe_2O_3				**0.58**	−0.05	−0.11	−0.07	0.10	−0.01	**0.72**	−0.31	0.32
MnO					**0.55**	**0.56**	−0.11	−0.07	0.10	0.23	0.33	−0.27
MgO						**0.98**	**−0.58**	−0.43	**0.87**	−0.35	**0.91**	−0.31
CaO							**−0.62**	−0.47	**0.82**	−0.42	**0.94**	−0.37
Na_2O								0.09	−0.40	0.19	**−0.63**	−0.01
K_2O									−0.29	−0.22	−0.24	**0.97**
P_2O_5										−0.33	**0.78**	−0.17
Cr_2O_3											**−0.68**	−0.09
LOI												−0.19

Correlation coefficients above 0.5 are written in bold. The full correlation matrix and significance of the correlation coefficient is provided in Supplementary Table S7

LOI, loss of ignition

Paleoclimatic conditions

Reconstructing the paleoclimate by using geochemical proxy signals of element ratios (Rb/K, V/Cr and Zr/Ti) assists in identifying relationships between the rocks' ARD (acid rock drainage) potential and the rock geochemistry resulting from paleoclimatic conditions. The Rb/K ratio is used as a salinity proxy to differentiate the environments from freshwater, brackish to marine environments, where marine environments have higher concentrations of Rb than freshwater environments (Scheffler et al. 2006). V/Cr is used as a proxy for redox conditions, where oxic conditions are indicated by ratios below 2, dysoxic conditions by ratios between 2 and 4.25 and anoxic conditions by ratios above 4.25 (Geel et al. 2013; Smithard et al. 2015). Finally, the Zr/Ti ratio is a provenance proxy, representing immobile elements during periods of weathering. The Zr/Ti ratio is thus of relevance because it considers whether the changes observed in the Whitehill Formation occur as a result of the influence of palaeoclimatic conditions or changes in the precursor rocks (Table 5). Rb/K ratios were found to be between 0.05 and 4.34, with the lowest ratio for sample CV and the highest one for LF1a. Samples LF2b, LB1 and LB2 indicate V/Cr ratios within oxic conditions; sample LF1a indicates dysoxic conditions; samples LF1b, LF2a and CV indicate anoxic palaeo-conditions. For Zr/

Table 3 Mineral assemblage of the Whitehill Formation samples based on the CIPW norm calculation

Mineral	LF1a	*LF1b*	*LF2a*	LF2b	*CV*	LB1	LB2
Quartz	47.39			6.44		87.9	45.49
Calcite	0.24	50.85	52.19	2.59	52.92	6.37	2.43
Olivine		33.07	30.85		37.37		
Plagioclase							48.33
Orthoclase	23.30			1.55		0.12	1.09
Hypersthene	2.58			20.92		1.93	0.44
Magnetite	3.45	3.10	3.86	7.95	0.20	2.46	0.88
Corundum	9.50	0.88	1.27	0.10	0.53	0.42	0.80
Ilmenite	0.97	0.08	0.09	1.54	0.04	0.02	0.23
Apatite	0.21	0.65	0.32	0.32	0.49	0.09	0.19
Kalsilite		0.43	0.49		0.18		
Chromite						0.04	

Weathered samples that resulted in acidic drainage in the batch experiments are in italics

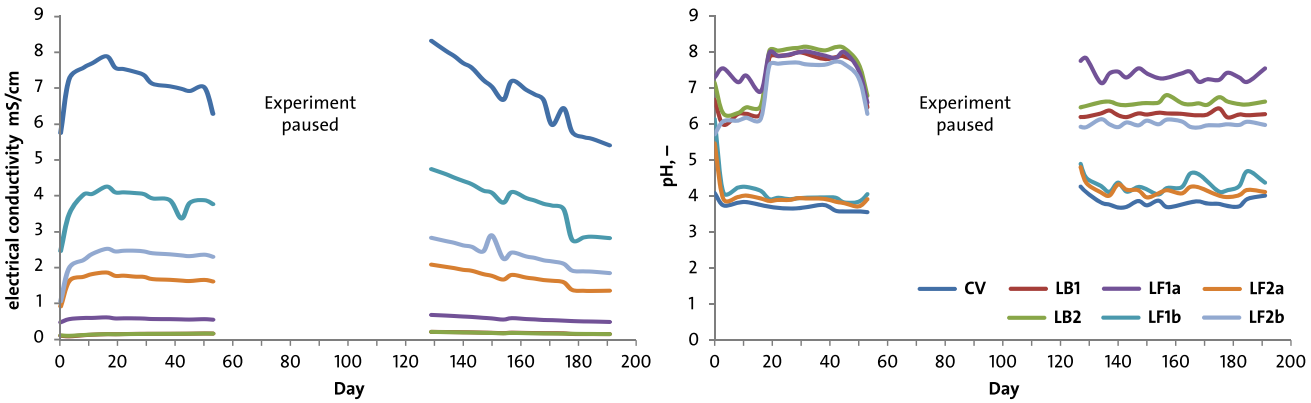

Fig. 9 Batch test results for electrical conductivity and pH of the seven samples. Samples LB1 and LB2 developed similar electrical conductivities and seem to be only one line

Ti ratios, all the samples have high ratios between 186 and 3283. The Zr/Ti ratio increased to higher values for samples LF1a and LB2 and was within the same range for the remaining samples.

High CIA values indicate intense chemical weathering because of the removal of alkali and alkaline earth elements. Low CIA values indicate partial chemical weathering due to higher feldspar content in the precursor rock (Scheffler et al. 2006). Results show that all CIA values were between 1.1 and 66 (Table 5), with sample LF1 having the highest CIA value, followed by samples LF2b and LB2, resulting from the leaching of mobile elements. Samples LF1b, LF2a, CV and LB1 have low CIA values indicating a decrease in chemical alteration processes and reduced leaching of mobile elements in the precursor rocks. One of the factors that promote slow weathering rates is the presence of minerals that are resistant to weathering, such as potassium feldspar or quartz (Al-Dabbagh et al. 2011; Goldberg and Humayun 2010).

Batch modelling of acid mine drainage environments

PHREEQC modelling of the ARD environment with the batch sample pH and water analysis results determines possible mineral equilibria and saturation indices of relevant phases (Table 6, Supplementary Figure S5). The saturation indices for the batch leaching samples of the Whitehill Formation show undersaturated ($SI \leq 0$) as well as supersaturated ($SI \geq 0$) phases (Table 6), the majority of those with $SI \in [-1, 1]$ being slightly undersaturated. Only the SiO_2-phases with slower kinetics are slightly oversaturated.

Table 4 Results of water analysis using ICP-MS, discrete analyser, as well as pH and electrical conductivity (EC) of the batch experiments

Parameter	LF1a	*LF1b*	*LF2a*	LF2b	*CV*	LB1	LB2
pH	7.17	4.40	4.05	6.00	3.87	6.22	7.78
EC	480	2840	1340	1870	5570	140	130
Al	< 0.10	7.40	4.84	< 0.10	24.0	< 0.10	0.23
B	0.02	< 0.20	0.10	< 0.20	0.28	0.02	0.02
Ca	108	614	209	606	608	23.0	39.0
Fe	< 0.03	0.03	< 0.03	< 0.03	0.04	< 0.03	< 0.03
K	38	29	23	18	41	2.4	5.6
Li	< 0.01	0.09	0.03	0.04	0.24	< 0.01	< 0.01
Mg	12	77	41	88	249	10	7
Mn	< 0.03	2.29	3.18	< 0.03	15	< 0.03	0.14
Na	6	314	180	28	1066	3	13
P	< 0.01	0.02	0.13	< 0.01	0.03	0.03	0.08
Si	3.7	15	28	3.7	43	1.4	12.0
Cl	45	458	231	91	1556	10	4
Alkalinity	66	− 178	− 72	16.4	− 241	78	153
F	0.50	0.30	0.60	0.40	0.20	0.20	0.20
NO_3^-	1.40	1.60	2.00	4.30	1.20	2.60	2.10
SO_4^{2-}	230	2191	877	1912	2803	13	4
Ion balance	0.92	− 0.88	− 0.54	− 0.90	− 0.69	1.13	0.05

Elements in mg/L, electrical conductivity (EC) in µS/cm, pH without unit, total alkalinity as HCO_3^- (mg/L), ion balance in %, negative alkalinity is acidity

Table 5 Ratio of the geochemical proxies and chemical index of alteration (CIA) values for seven samples of the Whitehill Formation

Sample	Rb/K	V/Cr		Zr/Ti	CIA
LF1a	4.34	2.95	Dysoxic	3283	66.0
LF1b	0.33	7.78	Anoxic	271	1.9
LF2a	0.61	8.39	Anoxic	392	2.6
LF2b	0.35	0.42	Oxic	194	39.7
CV	0.05	11.41	Anoxic	186	1.1
LB1	0.83	1.13	Oxic	200	6.3
LB2	0.52	0.54	Oxic	3000	46.1

Weathered samples resulting in acidic drainage in the batch experiments are in italics

Discussion

Geological conditions

The geological landscape between the three sites (LF1, LF2 and CV) investigated is compositionally similar, and the individual units can be correlated. Where gypsum occurs, it is dominant in weathered zones in connection with shale layers. This is likely to represent a zone of gypsum accumulation prompted by reactions between a pyrite-bearing rock and calcite or hydrogen carbonate fluids from the overlying shale. As the Whitehill Formation comprises organic-rich sediments, the complexation of the cations in these fluids and consequently their mobility will become increased. In this case, metals that would normally not be mobile under the prevailing Eh–pH conditions could move (Velde 1995). The reactions are likely initiated by percolating meteoric water and oxygen that enter the rock through fractures and veins. The gypsum layer underlying the near-surface shale bed is thickest in the whole sequence, and the lower shale bed has produced a thinner gypsum unit below it for location LF1. The lowermost shale unit has been unsuccessful in creating its own leached layer below it, thus leading to weathering. This continuous thinning of gypsum leachate with depth is also observed in location LF2. The distribution of gypsum and the thickness of the resulting layers are probably controlled by the frequency of dissolution of carbonaceous shales and the volume of solutions that percolate through the rock. However, the sequence in which the precipitates appear in the Whitehill Formation might differ for other sites that were not investigated. Authors such as Geel et al. (2013) have conducted petrographic studies on the shale layers of the Whitehill Formation and identified euhedral to framboidal pyrite grains. Breit and Wanty (1991) described the geochemical controls of carbonaceous rocks and pointed out that reducing conditions favour H_2S formation and V precipitation, which would explain why sections of the Whitehill Formation are anoxic (Table 5) and contain both elevated V concentrations and di-sulfide minerals. Therefore, it can

Table 6 Results of the PHREEQC geochemical modelling of the batch experiment water

Mineral phase	LF1a	*LF1b*	*LF2a*	LF2b	*CV*	LB1	LB2
Adularia ($KAlSi_3O_8$)	−0.62	–	–	–	–	−4.82	0.48
Aragonite ($CaCO_3$)	−0.58	–	–	–	–	−1.97	0.07
Calcite ($CaCO_3$)	−0.44	–	–	–	–	−1.83	0.22
Anhydrite ($CaSO_4$)	−1.36	−0.19	−0.78	−0.20	−0.78	−3.00	–
Gypsum ($CaSO_4.2H_2O$)	−1.14	0.02	−0.56	0.02	−0.56	−2.80	−3.13
Jurbanite ($AlOHSO_4$)	–	0.25	−0.26	−1.53	−0.26	−4.05	−7.11
Chalcedony (SiO_2)	−0.66	−0.04	0.22	−0.65	0.22	−1.08	−0.15
Cristobalite (SiO_2)	−0.62	−0.01	0.26	−0.62	0.26	−1.05	−0.12
Quartz (SiO_2)	−0.23	0.39	0.62	−0.22	0.65	−0.65	0.28
Silicagel (SiO_2)	−1.19	−0.58	−0.31	−1.19	−0.31	−1.61	−0.69

Saturation indices (SI) from water analysis of the Whitehill Formation. Only phases where at least one sample had SI∈[−1, 1] were selected; "–" indicates no SI calculated. Weathered samples resulting in acidic drainage in the batch experiments are in italics

be safely assumed that the weathering of pyrite in the presence of oxygenated water produced sulfuric acid and Fe oxyhydroxide precipitates. The acid produced in this reaction as well as the carbonic acid produced by water–CO_2 interaction leads to the dissolution of calcite in the presence of water, thus leading to solutions that are supersaturated with respect to gypsum. As Hem (1985) describes, shales are usually porous and might contain interstitial water with high mineralisation. Geel et al. (2013) has reported the presence of dolomite concretions between layers of the black shale, which indicates the chemical changes that result from the variation in pore water composition. In Laingsburg (Supplementary Figure S3) but also at the other two locations, dolomite concretions in the form of ovoid and elongate shapes were identified. Concretions form because of the bacterial oxidation of organic matter and the increase in alkalinity of sediment pore water. In this instance, a pyrite-rich layer had undergone a process of sulfate reduction and an increase in the alkalinity content to form dolomite concretions. Based on the geochemical data (Table 4), the SO_4^{2-}-concentration for samples in Laingsburg was very low and the relative increase in alkalinity for these samples favoured the precipitation of the dolomite concretions. Consequently, the supersaturation of the alkaline pore water relative to the dolomite phase caused an increase in the size of the concretions (Mavotchy et al. 2016), which has also been shown by the laboratory leaching experiments, with the majority of the samples producing a circum-neutral pH during the experiment.

Geochemical conditions

The bulk chemistry of both fresh and weathered rock samples (Tables 4 and 5) shows that the most abundant compounds in the rock were SiO_2 and Al_2O_3 for samples LF1a, LF2b, LB1 and LB2, and CaO and MgO for samples LF1b, LF2a and CV. LOI and Fe_2O_3 are the third and fourth most abundant parameters, with LOI representing the sum of organic matter, inorganic carbon, sulfur and water in crystalline form (Santisteban et al. 2004), and its difference resulting from the sulfur variation in the samples.

CaO and MgO show a positive correlation with LOI; however, a negative correlation with SiO_2 is also obvious from the PCA results. The LOI, as expected, shows high wt % for weathered samples and low wt % for fresh samples. Samples LF1a, LF2b, LB1 and LB2 contain CaO and MgO between 0 wt % and 10.21 wt %, which usually are the main constituents of calcite ($CaCO_3$) and dolomite ($CaMg(CO_3)_2$). Yet, the XRD results from the literature show low calcite concentrations for these fresh rock samples; therefore, the CaO and MgO are related to the gypsum and very likely dolomite, clay minerals or pyrite.

Most of the trace elements in the rocks are correlated with K_2O, which might indicate that they are sorbed to clay minerals (e.g. illite) in the rock samples, which could be proven to be the negative correlation of these trace elements with the LOI. Because the LOI, which is indicative of carbonates, correlates strongly with Ca, Mg and Sr, their abundance in the samples can safely be assumed. At first, the high negative correlation of the pH with the Ca, Mg and Sr in the rock samples seems to be contractionary. Yet, this results from the pyrite oxidation producing sulfuric acid and consequently dissolving the more soluble minerals in the rock, namely the carbonates.

Similar geochemical conditions to the Whitehill Formation are described by Baiyegunhi et al. (2018), Geel et al. (2015), Geel et al. (2013) and Smithard et al. (2015) in Loeriesfontein, Calvinia, Jansenville and other strata similar to the Whitehill Formation (Supplementary Table S8). These studies suggest that pyrite was oxidised, then reacted with the hydrogen carbonate fluids to form traces of gypsum.

However, no pyrite was identified during the field investigations for this study, but evidence of iron oxyhydroxide indicates that pyrite must have been oxidised, e.g. at Loeriesfontein (Fig. 5). The gypsum formation results from the weathering of pyrite, calcite and dolomite abundant in the Whitehill Formation, which produces solutions enriched in Fe, Ca, Mg and hydrogen carbonate once meteoric water or groundwater percolates through the rock. This corresponds with the XRF results of this and the other studies, which show CaO and SO_4^{2-}. When the thermodynamic conditions (oversaturation, pH and redox state) for the precipitation of gypsum or iron oxides are reached, both gypsum and iron oxides precipitate in fractures of the rock or on the surface of the rocks. As the batch experiments and modelling with PHREEQC showed, there is a clear correlation between the Ca content in the rocks and the Ca concentration in the water, resulting in a slight oversaturation of the fluids in relation to the species gypsum. Results from the PCA grouping of the XRF results and the hydrochemical development of the batch experiments show that the rocks' chemical composition clearly determines the pH and electrical conductivity development of the rock samples. Gypsum precipitates growing in veins, crystal masses or desert roses formed on the investigated sites. The geochemical proxy signals and the CIA values suggest that the rate at which these geochemical processes took place is very slow, under dysoxic and anoxic conditions. For example, changes from oxic to dysoxic conditions resulted in gypsum dissolution or gypsum being in equilibrium with the solution, whereas changes from oxic/dysoxic to anoxic conditions resulted in the precipitation of gypsum, which is relevant to this study.

Geochemical modelling

Results of geochemical modelling used to predict the long-term behaviour of AMD processes are considered relevant when they show similarities to the field observations (Alpers and Nordstrom 1999). Based on the results, the mineral dissolution and precipitation described the behaviour of SO_4^{2-}, Ca^{2+}, Mg^{2+} and other water constituents in mine water environments. The water–rock interactions are controlling the processes in AMD environments of the Witwatersrand Basin, resulting in the observed concentrations of SO_4^{2-} and Ca, which further influence mineral precipitation reactions and thus affect the mine water quality. Calcite and dolomite weathering under oxic conditions results in increased hydrogen carbonate, Ca^{2+} and Mg^{2+} concentrations in the solution. The Ca further reacts with SO_4^{2-} released from pyrite oxidation to precipitate as gypsum. In oxic mine water conditions, the concentration of SO_4^{2-} remains high and that of Ca^{2+} decreases as gypsum precipitates during the mine water's flow through fractures or pores. Secondary minerals form because of changes in pH and redox reactions. The concentration of Fe and SO_4^{2-} and dissolved semi-metals are controlled by the formation of secondary phases (Bain et al. 2000; Phan et al. 2018). When gypsum and Fe oxides precipitate, it results in immobilising Fe and SO_4^{2-}, which can be seen by the Fe oxyhydroxide and gypsum precipitates that have formed in the vicinity of the Whitehill and similar formations (Figs. 5 and 7).

Based on the Doctrine of Uniformity ("uniformitarianism"), changes in the earth's crust during geological history have resulted from the action of the continuous and uniform process. Thus, in the Witwatersrand Basin, the quality of mine water is controlled by water–rock interactions, similar to the processes in the Whitehill Formation (Table 7). High SO_4^{2-} concentrations (up to several thousand mg/L as shown in this study) persisted in the Whitehill Formation over millions of years, proving the immobility of the elements under reducing conditions. The mobility of elements is very unlikely because of the anoxic conditions which promote very slow rates of water–rock interactions in the Whitehill Formation. Thus, when gypsum precipitates, pyrite oxidation ceases until there is enough oxygen supply to allow the reaction to continue. Sulfate concentrations up to several thousand mg/L are common in mine waters in the Witwatersrand Basin. Based on the deductions drawn from the Whitehill Formation, analogous processes can be expected at the Witwatersrand Basin, resulting in the precipitation or dissolution of minerals, thus changing the quality of mine water. In consequence, this will reduce the sulfate concentration of the mine water, increase the mine water's pH and

Table 7 Comparison of Witwatersrand Basin mine water (Expert Team of the Inter-Ministerial Committee 2010) with the acidic fluids of the batch experiments

Parameter	Witwatersrand Basin			Whitehill Formation			
	WB*	CB*	EB*	LF1b	LF2a	LF2b	CV
pH, –	3.5	2.8	6.65	4.40	4.05	6.00	3.87
EC, µS/cm	5100	4670	2460	2840	1340	1870	5570
SO_4^{2-}, mg/L	4010	3700	1037	2191	877	1912	2803
Fe, mg/L	697	112	38	0.03	< 0.03	< 0.03	0.04

Fe concentrations from the batch experiments are low because the experiments' oxic conditions resulted in Fe precipitation

WB, Western Basin; *CB*, Central Basin; *EB*, Eastern Basin (pre-2010 samples and modelled water quality)

because of the saturation of the pore, ground and mine water in relation to the carbonates, the dissolution of carbonate rocks will slow down. Therefore, these results can be used for improved water quality predictions and decision-making in the Witwatersrand area.

Conclusions

Recapitulating, the results show that all rock samples exhibiting pH values in the Fe to Al buffer range during the batch experiments have gypsum in equilibrium with the laboratory solution. Reconstructing the paleoclimate using the CIA indicated that changes in the depositional environment between marine and freshwater environments and the consequent changes in redox conditions influenced the geochemical system which prevailed. The rocks of the Witwatersrand Basin are composed primarily of pyrite-bearing quartzites and quartz pebble conglomerates, which are, in places, located below a dolomite aquifer. Where acid mine drainage comes into contact with dolomite, characteristic concretions of gypsum and iron oxyhydroxide minerals form. Though the detailed geological conditions in the Whitehill Formation are not identical, particularly they consist of pyrite-bearing shale and dolomite concretions, these conditions also led to the formation of gypsum and iron oxyhydroxide precipitates after the geochemical reactions between water, oxygen and the di-sulfide minerals in the rock, which caused ARD. Using this knowledge of the geological settings, strata like the Whitehill Formation, the paleoclimate, geochemistry and PHREEQC modelling, it can be deduced that di-sulfide oxidation, as expected, generates protons, sulfate and ferrous iron as major ions. Due to the exposure to atmospheric conditions, oxidation of ferrous iron and subsequent hydrolysis of ferric iron occurs. The generated sulfate reacts with the Ca ions from carbonate weathering to (a) neutralise the solution and (b) precipitate gypsum. Consequently, during the passage of the mining influenced water through the pores or fractures of the strata in the Witwatersrand, the mine water will become less reactive, as has been shown in the natural analogue of the Whitehill Formation, where widespread ARD is not found today. In the presence of silica, silicate minerals might also precipitate. This assemblage of reactions and reaction products is commonly known as natural attenuation.

Using uniformitarianism and the geochemical processes of the water–rock interactions in the Whitehill Formation allows predicting how the mine water in the Witwatersrand Basin will evolve over the long term. Because the pore water in the Whitehill Formation, which results from pyrite weathering, can become oversaturated in relation to dolomite, this might also be expected for the Witwatersrand mine water. Once it gets into contact with the Malmani dolomite aquifer, the mine water will reach circum-neutral pH values and get saturated relative to the dolomite, therefore not dissolving it any further. Using this conclusion in more detailed modelling studies of the Whitehill Formation and transposing these results to the Witwatersrand Basins and other mining influenced areas will substantially contribute to understanding and improving AMD and MIW prediction methods (e.g. acid–base accounting or humidity tests) for the next generation of mine sites.

Supplementary Information The online version contains supplementary material available at https://doi.org/10.1007/s11356-021-17699-6.

Acknowledgements We thank the National Research Foundation (NRF, Grant UID 86948) under the SARChI programme for funding this project. David Khoza substantially improved the language, and Elke v. Hünefeld-Mugova found inconsistencies. Thanks to the Council for Geoscience for the chemical analysis of the rock samples. Thanks to Kagiso More and Corinna Schwarz for assisting in the field. CW thanks Emelie Waldken for keeping him tuned. We also thank the reviewers who helped to shape the paper with valuable comments.

References

Al-Dabbagh SM, Othman SM, Dhannoun HY (2011) The relationship between chemical index of alteration and some major and trace elements content in rocks of Injana Formation of Northern Iraq. Irq Nat J Chem 11(1):1–22

Alpers CN, Nordstrom DK (1999) Geochemical modelling of water-rock interactions in mining environments. In: Plumlee GS, Logsdon MJ (eds) The Environmental Geochemistry of Mineral Deposits, vol 6A. Society of Economic Geologists, Littleton, pp 289–323

Bain JG, Blowes DW, Robertson WD, Frind EO (2000) Modelling of sulfide oxidation with reactive transport at a mine drainage site. J Contam Hydrol 41(1–2):23–47. https://doi.org/10.1016/S0169-7722(99)00069-8

Baiyegunhi C, Liu KW, Wagner N, Gwavava O, Oloniniyi TL (2018) Geochemical evaluation of the Permian Ecca Shale in Eastern Cape Province, South Africa: implications for shale gas potential. Acta Geol Sin Engl 92(3):1193–1217. https://doi.org/10.1111/1755-6724.13599

Berner RA (1980) Early diagenesis – a theoretical approach. Princeton series in geochemistry. Princeton University Press, Princeton

Boukhalfa C, Chaguer M (2012) Characterisation of sediments polluted by acid mine drainage in the northeast of Algeria. Int J Sediment Res 27(3):402–407. https://doi.org/10.1016/S1001-6279(12)60045-6

Breit GN, Wanty RB (1991) Vanadium accumulation in carbonaceous rocks: a review of geochemical controls during deposition and diagenesis. Chem Geol 91(2):83–97. https://doi.org/10.1016/0009-2541(91)90083-4

Bruner KR, Smosna R (2011) A comparative study of the Mississippian Barnett Shale, Fort Worth Basin, and Devonian Marcellus Shale, Appalachian Basin, Report № DOE/NETL-2011/1478. United States Department of Energy, Albany, 106 p

Chapman RE (1981) Geology and water – an introduction to fluid mechanics for geologists. Developments in Applied Earth Sciences, vol 1. Nijhoff Junk, The Hague

Choi BY, Yun ST, Mayer B, Hong SY, Kim KH, Jo HY (2012) Hydrogeochemical processes in clastic sedimentary rocks, South Korea

– a natural analogue study of the role of dedolomitization in geologic carbon storage. Chem Geol 306–307:103–113. https://doi.org/10.1016/j.chemgeo.2012.03.002

Chukwuma K, Bordy EM (2016) Spatiotemporal sedimentary facies variations in the Lower Permian Whitehill Formation, Ecca Group, Karoo Basin. In: Linol B, de Wit MJ (eds) Origin and Evolution of the Cape Mountains and Karoo Basin. Springer, Cham, p 101–110. https://doi.org/10.1007/978-3-319-40859-0_10

Coetzee H (2013) Flooding of the underground mine workings of the Witwatersrand Gold Fields. In: Brown A, Figueroa L, Wolkersdorfer C (eds) Reliable Mine Water Technology. International Mine Water Association, Golden, p 937–942

Crawford J (1999) Geochemical modelling – a review of current capabilities and future directions. SNV Report 262:1–39

Department of Water Affairs and Forestry South Africa (2009) Vaal river system: large bulk water supply reconciliation strategy: second stage reconciliation strategy (March 2009), Report № P RSA C000/00/4406/08. Department of Water Affairs and Forestry, Pretoria, 90 p

Doveton JH (2018) Mathematical minerals: a history of petrophysical petrography. In: Daya Sagar BS, Cheng Q, Agterberg F (eds) Handbook of Mathematical Geosciences: Fifty Years of IAMG. Springer, Cham, p 467–481. https://doi.org/10.1007/978-3-319-78999-6_24

Enomoto CB, Coleman JL Jr, Haynes JT, Whitmeyer SJ, McDowell RR, Lewis JE, Spear TP, Swezey CS (2012) Geology of the Devonian Marcellus shale Valley and Ridge Province, Virginia and West Virginia – a field trip guidebook for the American Association of Petroleum Geologists Eastern Section Meeting. U S Geol Surv Open File Rep 2012–1194:1–48. https://doi.org/10.3133/ofr20121194

Expert Team of the Inter-Ministerial Committee (2010) Mine water management in the Witwatersrand Gold Fields with special emphasis on acid mine drainage – report to the Inter-Ministerial Committee on Acid Mine Drainage. Council for Geoscience, Pretoria

Geel C, Schulz H-M, Booth P, deWit M, Horsfield B (2013) Shale gas characteristics of Permian Black Shales in South Africa: results from recent drilling in the Ecca group (Eastern Cape). Energy Procedia 40:256–265. https://doi.org/10.1016/j.egypro.2013.08.030

Geel C, De Wit M, Booth P, Schulz H-M, Horsfield B (2015) Palaeoenvironment, diagenesis and characteristics of Permian Black Shales in the Lower Karoo Supergroup Flanking the Cape Fold Belt near Jansenville, Eastern Cape, South Africa: implications for the shale gas potential of the Karoo Basin. S Afr J Geol 118(3):249–274. https://doi.org/10.2113/gssajg.118.3.249

Geller W, Klapper H, Salomons W (1998) Acidic mining lakes – acid mine drainage, limnology and reclamation. Springer, Berlin

Goldberg K, Humayun M (2010) The applicability of the Chemical Index of Alteration as a paleoclimatic indicator: an example from the Permian of the Paraná Basin, Brazil. Palaeogeogr Palaeoclimatol Palaeoecol 293(1):175–183. https://doi.org/10.1016/j.palaeo.2010.05.015

Hammer Ø, Harper DAT, Ryan PD (2001) PAST – paleontological statistics software package for education and data analysis. Palaeontol Electronica 4(1):1–9

Hem JD (1985) Study and interpretation of the chemical characteristics of natural water. US Geol Surv Water Suppl Pap 2254:263. https://doi.org/10.3133/wsp2254

Hobbs PJ, Cobbing JE (2007) A hydrogeological assessment of acid mine drainage impacts in the West Rand Basin, Gauteng Province, Report № CSIR/NRE/WR/ER/2007/0097/C. Council for Scientific and Industrial Research Natural Resources & the Environment, Pretoria, 59 p

Hobbs PJ, Jamison A, Leyland R, Venter J, Roelofse F, Coetzee H, Wade P, Hardwick D, Butler M, Abiye T, Verhagen BT (2011) Situation Assessment of the surface water and groundwater resource environments in the cradle of Humankind World Heritage Site, Report № BIQ005/2008. Council for Scientific and Industrial Research, Council for Geoscience, Wits School of Geoscience, iThemba LABS, A. Jamison, D. Hardwick, Johannesburg, 238 p

Hobbs PJ (2008) Situation analysis of hydrologic and hydrogeologic factors informing the royal engineering groundwater supply on Sterkfontein 173IQ, Krugersdorp, Report № CSIR/NRE/WR/ER/2008/0107/C. Council for Scientific and Industrial Research Natural Resources & the Environment, Pretoria

Jacobs JA, Lehr JH, Testa SM (2014) Acid mine drainage, rock drainage, and acid sulfate soils – causes, assessment, prediction, prevention, and remediation. Wiley, Hoboken

Jambor JL, Nordstrom DK, Alpers CN (2000) Metal-sulfate salts from sulfide mineral oxidation. Rev Mineral Geochem 40(1):303–350. https://doi.org/10.2138/rmg.2000.40.6

Johnson MR, Anhaeusser CR, Thomas RJ (2006) The geology of South Africa. Council for Geoscience, Pretoria

Kern ML, Vieiro AP, Machado G (2008) The fluoride in the groundwater of Guarani Aquifer System: the origin associated with black shales of Paraná Basin. Environ Geol 55:1219–1233. https://doi.org/10.1007/s00254-007-1067-1

Kesserü Z (1994) Utilising the experience of mine water engineering for siting deep waste repositories. Proceedings, 5th International Mine Water Congress, Nottingham, UK 2:715-726

Le Maitre RW, Streckeisen A, Zanettin B, Le Bas MJ, Bonin B, Bateman P, Bellieni G, Dudek A, Efremova S, Keller J, Lameyre J, Sabine PA, Schmid R, Sorensen H, Woolley AR (2002) Igneous rocks – a classification and glossary of terms. 2nd edn. Cambridge University Press, Cambridge

Liang-qi L, Ci-an S, Xiang-li X, Yan-hong L, Fei W (2010) Acid mine drainage and heavy metal contamination in groundwater of metal sulfide mine at arid territory (BS mine, Western Australia). Trans Nonferrous Met Soc China 20(8):1488–1493. https://doi.org/10.1016/S1003-6326(09)60326-5

Libourel G, Carron AV, Morlok A, Gin S, Sterpenich J, Michelin A, Neff D, Dillmann P (2011) The use of natural and archeological analogues for understanding the long-term behaviour of nuclear glasses. Geoscience 343(2–3):237–245. https://doi.org/10.1016/j.crte.2010.12.004

Mathur R, Jun L, Prush V, Paul J, Ebersole C, Fornadel A, Williams JZ, Brantley S (2012) Cu isotope and concentrations during weathering of black shale of the Marcellus Formation, Huntington County, Pennsylvania (USA). Chem Geol 304–305:175–184. https://doi.org/10.1016/j.chemgeo.2012.02.015

Mavotchy NO, El Albani A, Trentesaux A, Fontaine C, Pierson-Wickmann AC, Boulvais P, Riboulleau A, Pemba LN, Pambo F, Gauthier-Lafaye F (2016) The role of the early diagenetic dolomitic concretions in the preservation of the 2.1-Ga paleoenvironmental signal: the paleoproterozoic of the Franceville Basin, Gabon. CR Geosci 348(8):609–618. https://doi.org/10.1016/j.crte.2016.08.002

McCarthy TS (2006) The Witwatersrand Supergroup. In: Johnson MR, Anhaeusser CR, Thomas RJ (eds) The geology of South Africa. Geological Society of South Africa, Council for Geoscience, Johannesburg, Pretoria, p 155–186

McCarthy TS (2011) The impact of acid mine drainage in South Africa. S Afr J Sci 107(5/6):712(1–7). https://doi.org/10.4102/sajs.v107i5/6.712

McLachlan IR, Anderson AM (1977) Fossil insect wings from the early Permian white band formation, South Africa. Palaeont Afr 20:83–86

Miller W, Alexander R, Chapman N, McKinley I, Smellie J (2000) Natural analogue studies in the geological disposal of radioactive wastes. Waste Management Series, vol 2. Pergamon, Amsterdam

Naicker K, Cukrowska E, McCarthy TS (2003) Acid mine drainage arising from gold mining activity in Johannesburg, South Africa and environs. Environ Pollut 122(1):29–40. https://doi.org/10.1016/S0269-7491(02)00281-6

Nesbitt HW, Markovics G (1997) Weathering of granodioritic crust, long-term storage of elements in weathering profiles, and petrogenesis of siliciclastic sediments. Geochim Cosmochim Acta 61(8):1653–1670. https://doi.org/10.1016/S0016-7037(97)00031-8

Nesbitt HW, Young GM (1982) Early proterozoic climates and plate motions inferred from major element chemistry of lutites. Nature 299(5885):715–717. https://doi.org/10.1038/299715a0

Nesbitt HW, Young GM (1989) Formation and diagenesis of weathering profiles. J Geol 97(2):129–147. https://doi.org/10.1086/629290

Oelofsen BW (1987) The biostratigraphy and fossils of the Whitehill and Irati Shale Formations of the Karoo and Paraná Basins. In: McKenzie GD (ed) Gondwana Six: Stratigraphy, Sedimentology, and Paleontology. vol 41. American Geophysical Union, Washington, p 131–138. https://doi.org/10.1029/GM041p0131

Parkhurst DL, Appelo CAJ (2013) Description of input and examples for PHREEQC version 3 – a computer program for speciation, batch-reaction, one-dimensional transport, and inverse geochemical calculations. US Geol Surv Tech Methods 6(A43):1–497. https://doi.org/10.3133/tm6A43

Phan TT, Paukert Vankeuren AN, Hakala JA (2018) Role of water–rock interaction in the geochemical evolution of Marcellus Shale produced waters. Int J Coal Geol 191:95–111. https://doi.org/10.1016/j.coal.2018.02.014

Pruseth KL (2009) Calculation of the CIPW norm: new formulas. J Earth Syst Sci 118(1):101–113. https://doi.org/10.1007/s12040-009-0010-0

Republic of South Africa, Department of Water Affairs and Forestry (2004) National Water Resource Strategy (NWRS). Department of Water Affairs and Forestry, Pretoria, p 150

Rimmer SM (2004) Geochemical paleoredox indicators in Devonian-Mississippian black shales, Central Appalachian Basin (USA). Chem Geol 206(3–4):373–391. https://doi.org/10.1016/j.chemgeo.2003.12.029

Santisteban JI, Mediavilla R, López-Pamo E, Dabrio CJ, Zapata MBR, García MJG, Castaño S, Martínez-Alfaro PE (2004) Loss on ignition: a qualitative or quantitative method for organic matter and carbonate mineral content in sediments? J Paleolimnol 32(3):287–299. https://doi.org/10.1023/B:JOPL.0000042999.30131.5b

Scheffler K, Buehmann D, Schwark L (2006) Analysis of late Palaeozoic glacial to postglacial sedimentary successions in South Africa by geochemical proxies – response to climate evolution and sedimentary environment. Palaeogeogr Palaeoclimatol Palaeoecol 240(1):184–203. https://doi.org/10.1016/j.palaeo.2006.03.059

Selley RC (2000) Applied sedimentology. 2nd edn. Academic Press, San Diego

Singer PC, Stumm W (1970) Acidic mine drainage – the rate-determining step. Science 167(3921):1121–1123. https://doi.org/10.1126/science.167.3921.1121

Smellie JAT, Karlsson F, Alexander WR (1997) Natural analogue studies: present status and performance assessment implications. J Contam Hydrol 26(1):3–17. https://doi.org/10.1016/S0169-7722(96)00053-8

Smithard T, Bordy EM, Reid D (2015) The effect of dolerite intrusions on the hydrocarbon potential of the lower Permian Whitehill Formation (Karoo Supergroup) in South Africa and Southern Namibia: a preliminary study. S Afr J Geol 118(4):489–510. https://doi.org/10.2113/gssajg.118.4.489

Soares MB (2003) A taphonomic model for the Mesosauridae assemblage of the Irati Formation (Paraná Basin, Brazil). Geol Acta 1(4):349–361. https://doi.org/10.1344/105.000001621

Stumm W, Morgan JJ (1996) Aquatic chemistry – chemical equilibria and rates in natural waters. 3rd edn. Wiley & Sons, New York

Velde B (1995) Origin and mineralogy of clays – clays and the environment. Springer, Berlin

Wolkersdorfer C, Nordstrom DK, Beckie R, Cicerone DS, Elliot T, Edraki M, Valente TM, França SCA, Kumar P, Oyarzún Lucero RA, Soler AIG (2020) Guidance for the integrated use of hydrological, geochemical, and isotopic tools in mining operations. Mine Water Environ 39(2):204–228. https://doi.org/10.1007/s10230-020-00666-x

Wolkersdorfer C (2008) Water management at abandoned flooded underground mines – fundamentals, tracer tests, modelling, water treatment. Springer, Heidelberg

Younger PL, Banwart SA, Hedin RS (2002) Mine water – hydrology, pollution, remediation. Kluwer, Dordrecht